The photon-induced reactions of chemisorbed CH_3Br on Pt{111}

Cite as: J. Chem. Phys. **95**, 3930 (1991); https://doi.org/10.1063/1.460799
Submitted: 02 May 1991 • Accepted: 11 June 1991 • Published Online: 04 June 1998

G. Radhakrishnan, W. Stenzel, R. Hemmen, et al.

The photon-induced reactions of chemisorbed CH_3Br on Pt{111}

G. Radhakrishnan,[a] W. Stenzel, R. Hemmen, H. Conrad, and A. M. Bradshaw
Fritz-Haber-Institut der Max-Planck-Gesellschaft Faradayweg 4-6, W-1000 Berlin 33, Federal Republic of Germany

(Received 2 May 1991; accepted 11 June 1991)

The photochemistry of chemisorbed CH_3Br on Pt{111} has been investigated using high resolution electron energy loss spectroscopy (HREELS) and thermal desorption. The primary photon-induced reaction involves the cleavage of the C–Br bond, giving rise to chemisorbed CH_3 and Br, both of which can be identified in HREELS. From the angular dependence of the loss peaks, the symmetry of the CH_3 surface complex is shown to be C_{3v}. HBr can also be identified in subsequent thermal desorption. Experiments performed directly with HBr on Pt{111} indicate that molecular HBr adsorbs dissociatively on this surface. This result, in combination with observations of the C–H vibrational mode as a function of temperature, shows that the production of HBr arises from a secondary surface reaction between Br and CH_x fragments. Based on the wavelength dependence of the fragmentation cross section and the photoemission spectrum of adsorbed CH_3Br the primary photon-induced reaction to a charge transfer excitation is ascribed.

I. INTRODUCTION

Gas-surface reactions induced by lasers in the visible and near ultraviolet (UV) spectral regions have gained increasing importance in recent years in the technologically relevant areas of photo-induced etching, photoablation, and photo-induced growth of metal and compound-semiconductor thin films. A prerequisite for the optimization of such processes is the basic understanding of reaction pathways and mechanisms on well-characterized surfaces. Fundamental research in this field evolved with the study of photoreactions of adsorbed molecules on semiconductor and insulator surfaces.[1–6] More recently, however, photon-induced processes on metal surfaces have received considerable attention.

The photon-induced fragmentation of chemisorbed alkyl halides has been investigated by several groups.[3,4,7–12] In particular, White and co-workers have carried out a series of investigations on the adsorption, desorption, and decomposition of chloro-, bromo-, and iodo-methanes on Pt{111}.[7–9] These authors have shown that while CH_3I decomposes thermally, both CH_3Cl and CH_3Br dissociate only in the presence of UV photons. Whereas the mechanism of photon-induced dissociation of these chemisorbed systems is still under discussion, a photochemical dissociation pathway, identical to that in gas phase, has been favored by White *et al.* for the dissociation of CH_3Br on Pt{111}.[9] For this system it has been suggested that UV absorption by the adsorbed CH_3Br molecule leads to formation of an electronically excited state that is strongly repulsive with respect to the C–Br bond, resulting in direct dissociation. In work on coadsorbed CH_3Cl and CD_3Br,[8] both a direct excitation model, as well as a mechanism involving absorption in the metal, have been discussed. In the latter, photoelectrons or hot electrons are produced that cause dissociation via electron attachment to the adsorbate.

In the systems CH_3Br and CH_3Cl on Ni{111},[11,12] Marsh *et al.* have proposed a different fragmentation mechanism. For the dissociation of CH_3Br on Ni{111} at 193 nm, charge transfer processes between the substrate and the molecule have been suggested as the dominant step in the photochemistry.[11] Two fragmentation processes, namely, direct photofragmentation and dissociative electron attachment were thought to be responsible for the dissociation of CH_3Cl with 193 nm light, while at 248 nm the dissociation was attributed only to electron attachment.[12]

In addition to the work on alkyl halides, several other chemisorbed molecules have been studied. Chuang and Domen[13] have investigated the systems CH_2I_2/Al_2O_3 and CH_2I_2/Ag. Desorption associated with photon-induced fragmentation was monitored by x-ray photoemission, time-of-flight mass spectrometry, and thermal desorption. On both surfaces low quantum yields for dissociation were found indicating rapid electronic relaxation of the adsorbate. The photochemistry of ketene adsorbed on Pt{111} and also that of O_2 on Pt{111} have recently been investigated.[14,15] In studies on the decomposition of $Mo(CO)_6$ on Si{100},[16] and the decomposition and desorption of several metal carbonyls on Si{111},[17] the UV dissociation of the metal carbonyls has been attributed to an electronic excitation in the carbonyl. Hasselbrink and co-workers[18] have reported the photodissociation of NO_2 adsorbed on top of NO-saturated Pd{111}. These authors have concluded from the polarization dependence of the incident light that the photodissociation is caused by excitation of metal electrons rather than direct absorption in the adsorbate.

While no single mechanism for photo-induced dissociation processes on surfaces has been uniquely established, several reaction mechanisms have been discussed, as mentioned above. The photochemistry of adsorbates is complicated, compared to that of free molecules, by the presence of substrate electrons. It is generally expected that the excitation in the adsorbate can be rapidly quenched by energy transfer into the continuum of electronic excitations in the substrate. Lifetimes of repulsive states in the adsorbate may, however,

[a] Present address: The Aerospace Corporation, MS M2-241, P.O. Box 92957, Los Angeles, California 90009.

 0021-9606/91/183930-09$03.00

still be long enough to cause reaction before being quenched. An additional dissipative channel at surfaces is provided by a very effective coupling to surface and bulk phonon excitations, which may strongly influence a reaction coordinate in comparison to gas phase measurements. In almost all previous studies a comprehensive discussion of the mechanism of photon-induced processes in molecules chemisorbed on metal surfaces has been prevented by the lack of quantitative information in cross sections as well as by a severely restricted wavelength range.

In an earlier paper,[19] we reported the results of quantitative measurements made over a range of wavelengths in the near ultraviolet, establishing the fragmentation cross section of chemisorbed CH_3Br on Pt{111}. In this paper we focus primarily on understanding the chemical aspects of this system. In particular, high resolution electron energy loss spectroscopy (HREELS) has been used to characterize the vibrations of adsorbed species on the Pt{111} surface both before and after UV illumination. These measurements are complemented by thermal desorption spectroscopy (TDS) to monitor the products of the photon-induced reaction. Not only the primary reaction involving the cleavage of the C–Br bond, but also the secondary surface reaction resulting in the production of HBr at high temperatures have been followed with EELS. Finally, we contribute some more thoughts on the nature of the excitation mechanism of the primary photon-induced reaction.

II. EXPERIMENT

All experiments were carried out in a UHV chamber with a base pressure of 2×10^{-10} Torr. A Pt{111} crystal (area ~1 cm^2) was mounted between a pair of tungsten wires that were connected via a copper rod directly to a liquid nitrogen reservoir. The temperature of the directly heated crystal was measured with a chromel–alumel thermocouple welded to the back surface of the crystal. The sample surface was cleaned by cycles of Ar-ion bombardment (beam energy of 0.5 kV, 15 μA emission current) at room temperature and at 900 K. Following sputtering, the crystal was annealed at 1100 K for at least three minutes at a background pressure in the 10^{-9} Torr range.

Methyl bromide (99.5%, Linde) was used directly from a lecture bottle without further purification. Its purity was verified by the mass spectrometer. Two alternative methods, both yielding the same results, were used to prepare a monolayer of CH_3Br. The first method involved cooling the Pt{111} crystal to 160 K and then exposing it to CH_3Br at a typical dosage of 10^{-7} Torr for 50 s. Alternatively, the procedure suggested by White and co-workers was used. In this case, the sample was cooled to 148 K, which in our system was the lowest temperature attainable, followed by exposure to CH_3Br and then heating to 160 K. Since multilayers of CH_3Br desorb at 130 K, condensation does not occur. The monolayer desorbs at 165 K.

Irradiation of the Pt{111} crystal was performed in the upper level of the UHV chamber. The source of UV photons was a 1000 W high-pressure Xe lamp (LTI, LPS 1000*X*). The spectral power density distribution of the output of the Xe lamp including the collimating optics was experimentally determined by passing the output through a one-fourth meter monochromator (AMPCO Metrospec) and measuring the power with a calibrated power meter (Scientech 362) positioned at the exit slit. Entrance and exit slits of the monochromator were 20 mm long and their widths were 1 and 5 mm, respectively. The spectral bandpass under these conditions was 30 nm. Power measurements were made for a lamp input power of 760 W. These data were scaled accordingly for the appropriate lamp powers used during irradiation, assuming a linear scaling of output and input powers.

After passing through a water filter to eliminate unwanted infrared radiation, the output from the lamp was collimated with a telescope system comprising of 2 UV grade plano-convex lenses. All measurements reported here were made with the UV light at normal incidence. The collimated beam entered the UHV chamber through a port fitted with a MgF_2 window and illuminated the entire area of the sample uniformly. A set of short wavelength cutoff filters (Schott, WG 280 through GG 395) with precisely known transmission functions and with their short wavelength cutoffs ranging from 270 to 370 nm were used to perform wavelength selective UV irradiation. Typical irradiation times, starting at 148 K, were 40 min during which a 5–6 K increase in sample temperature is measured. This increase in temperature during irradiation is, however, still well below the desorption temperature of the monolayer. Between consecutive runs, it was made certain that the liquid nitrogen in the manipulator reservoir was boiled off, so as to prevent any readsorption of methyl bromide onto the Pt substrate from the cooled tube.

For TDS, the sample was resistively heated at a heating rate of 4 K/s from the lowest temperature of 148 K to as high as 1100 K. A Balzers (QMG 420) quadrupole mass spectrometer, mounted in one of the ports in the upper level of the chamber and directly viewing the illuminated sample surface, was used for these measurements. Control experiments with the sample surface rotated away from the mass spectrometer head enabled the products desorbing from the surface to be assigned uniquely.

The lower level of the chamber is equipped with a HREELS system, the design of which has been described elsewhere.[20] All HREELS spectra reported in this paper were acquired at a primary energy of 1.3 eV and an incidence angle of 55° from the surface normal. The typical resolution was 10–11 meV.

III. RESULTS AND DISCUSSION

A. Time dependence of the photon-induced reaction

In all our experiments both HBr (*m/e* 80) and Br (*m/e* 79) were detected in TDS after irradiation. Although CH_4 (*m/e* 16) was also detected, the detection of the higher masses 79 and 80 was preferred for the quantitative measurements, due to a large background of CH_4 present in the chamber. No measurable signals corresponding to Br_2 (*m/e* 158 or $PtBr^{++}$ (*m/e* 137) were observed. The dependence on UV illumination time has been studied both quantitatively with the thermal desorption spectra of Br and HBr, as well as qualitatively with the EEL spectra. Figure 1 shows plots

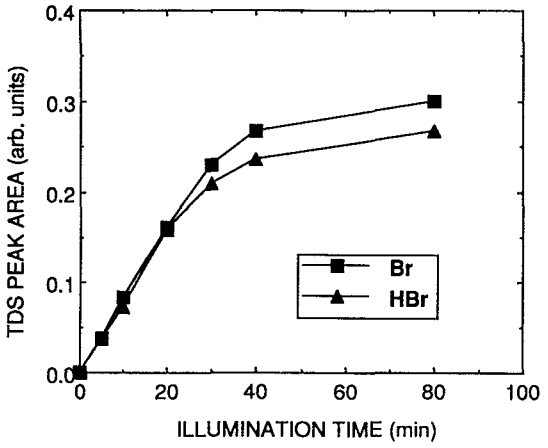

FIG. 1. Time dependence of fragmentation yields obtained from the Br and HBr signals in TDS.

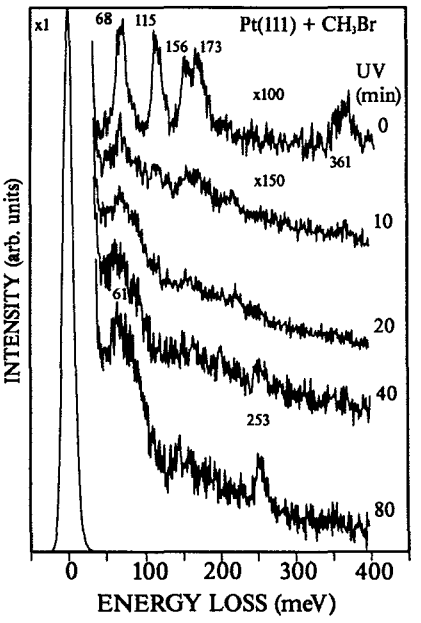

FIG. 2. HREEL spectra of chemisorbed CH_3Br as a function of illumination time. The different vibrational losses in the spectrum of the unilluminated parent molecule (time = 0) are listed in Table I. All spectra are measured in the specular direction and scaled with respect to the elastic peak (×1).

for the total areas of the Br and HBr thermal desorption peaks as a function of illumination time and indicates that after 40 min of illumination, the photolysis of a chemisorbed CH_3Br monolayer is nearly complete.

Figure 2 shows a corresponding series of EEL spectra, in the specular direction, as a function of increasing illumination time (0–80 min). The different loss peaks observed for the parent molecule (68, 115, 156, 173, and 361 meV) prior to UV illumination (time = 0) correspond to the different C–H vibrations and are discussed in detail in Sec. III D. The important point to note is that these spectra give qualitatively the same information as the thermal desorption spectra in Fig. 1. It can be clearly seen that after 10 min of illumination, the EEL spectrum still shows all the features characteristic of the parent molecule, although the loss peaks are significantly reduced in intensity. After 20 min of illumination the EEL spectrum begins to look markedly different with the CH_3 vibrations no longer observable. In addition, it can be seen that as the illumination time is increased, the C–Br stretch frequency (68 meV) begins to disappear and is instead replaced by the Pt–C stretch frequency (61 meV). When the illumination time is doubled from 40 to 80 min, there are no further significant alterations in the spectra. A loss peak at 253 meV is also observed, especially after 40 and 80 min of illumination, and is also discussed in Sec. III D.

B. Wavelength dependence of the photon-induced reaction

For the evaluation of fragmentation cross sections of chemisorbed CH_3Br on Pt{111}, a whole series of measurements was carried out, in which the sample was illuminated for 40 min with selected ranges of UV light from the Xe lamp using a set of cutoff filters. In each of these experiments, the illumination was followed by TDS measurements of HBr (m/e 80) and Br (m/e 79), which both show rather broad temperature maxima at 540 and 860 K, respectively. These results are shown in Fig. 3. It can be easily observed that the measurement with the full-arc [Fig. 3(a)] produces the largest desorption signals for both HBr and Br and that these signals decrease monotonically in intensity [Figs. 3(b)–3(f)] as the shorter wavelengths are eliminated.

In the full-arc illumination, the short wavelength cutoff is taken as 200 nm, the convoluted limit imposed by the rapidly decreasing lamp output and the transmission of all the optics. In all other measurements, the short wavelength cutoff is determined by the respective filter. The long wavelength cutoff was determined experimentally. With the cutoff filter GG 400 having no transmission below 390 nm, no measurable signals of HBr and Br were obtained in TDS, in spite of the fact that the total number of photons available from the lamp at $\lambda > 390$ nm is much greater than that below 390 nm. This clearly indicated that the absorption cross section of chemisorbed CH_3Br at $\lambda > 390$ nm must be negligibly small and allows the long wavelength cutoff to be placed at ~ 390 nm.

Complementary to the TDS data shown in Fig. 3, HREELS measurements also revealed a distinct dependence on the input photon wavelength. The loss peaks due to the resulting CH_3 fragment will be discussed later. It suffices here to note that they also decrease monotonically in intensity as the high energy photons are eliminated.

C. Fragmentation cross sections

Calculations of fragmentation cross sections were made using TDS data obtained with several different cutoff filters (Fig. 3). Details of the method used have been described elsewhere.[19] Briefly, beginning with the Beer–Lambert equation analogous to the gas phase, it is possible to correlate the TDS areas $N_d(j)$, obtained for each of the optical filters (j) in the wavelength interval i, to the dissociation or photofragmentation cross section $\sigma_d(i)$, the photon flux I_{ij}, the

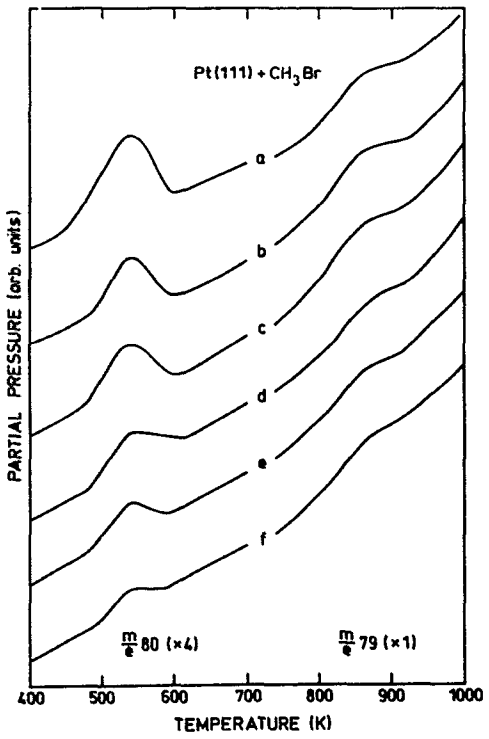

FIG. 3. TDS spectra of HBr (m/e 80) and Br (m/e 79) obtained with a series of optical filters after UV illumination of a chemisorbed monolayer of CH_3Br. (a) No filter, (b)–(f) cutoff wavelength λ at 290, 310, 320, 340, and 360 nm, respectively. No measurable signal was obtained with a filter having a cutoff wavelength at 390 nm.

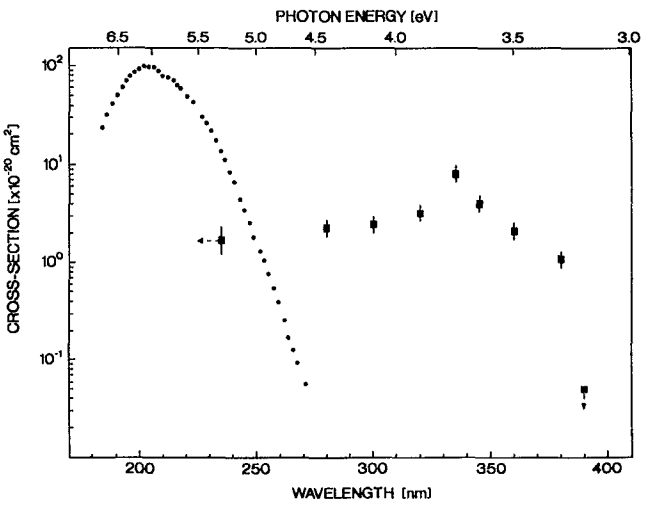

FIG. 4. Fragmentation cross section of chemisorbed CH_3Br calculated from the TDS data of m/e 79 for Fig. 3. Also shown is the gas-phase absorption cross section of CH_3Br taken from Ref. 21. The downward arrow on the cross section at 390 nm indicates that the value here represents our lower detection limit. The data point at 235 nm has been calculated for a rather large $d\lambda$ (200–280 nm), due to lack of filters at $\lambda < 280$ nm (unlike all other data for which $d\lambda$ is 10 or 20 nm). This uncertainty in wavelength is indicated by a horizontal arrow.

TDS area obtained with the entire range of available photons N_0, and the area of the sample A.

For purposes of the calculation it is assumed that the TDS area corresponding to 40 min of illumination without any filter [Fig. 3(a)] is proportional to the total number of dissociated molecules, and therefore to the total number of CH_3Br molecules initially adsorbed N_0. This assumption is justified, based on the time dependence studies described in Sec. III A. It has also been established that, for the exposures of CH_3Br used, the coverage is about one monolayer. This allows us to relate the density of CH_3Br molecules per unit area, ρ to N_0, the total number of dissociated molecules formed from one monolayer in the entire spectral range:

$$N_0 = C \times \rho \times A. \tag{1}$$

Because of this scaling, the absolute number of molecules at N_0 coverage is irrelevant. In addition, it is important to note that we approximate ρ as being constant in time, which is valid due to the experimentally observed linearity in Fig. 1. The final result is

$$N_d(j) = \Sigma_i I_{ij} N_0 \sigma_d(i)/A. \tag{2}$$

A direct analytical solution of (2) does not yield meaningful values for all the $\sigma_d(i)$, which is due to the experimental uncertainties in determining $N_d(j)$ with filters that produce the smallest TDS areas. A set of $\sigma_d(i)$'s from (2) was therefore empirically determined by an optimum set of $\sigma_d(i)$ that gave the best fit to the experimental values of $N_d(j)$'s. These data are plotted in Fig. 4. Also shown is a plot of the gas phase absorption cross section of CH_3Br in the wavelength range 180–250 nm.[21,22] As can be clearly seen by a comparison of these two curves, the fragmentation cross section obtained for chemisorbed CH_3Br is considerably broadened compared to the gas-phase absorption curve, and extends to nearly 400 nm. In addition, it displays a maximum in the range of 330–340 nm with a value of about 8×10^{-20} cm^2. The significance of these data of our understanding of the fragmentation mechanism is taken up again in Sec. III E.

D. Identification of parent and product vibrations using HREELS

1. CH_3Br

In Fig. 5 we present the HREEL spectra for monolayer CH_3Br measured in the specular and off-specular direction. Table I lists the vibrational frequencies corresponding to all the loss peaks observed in these spectra and the corresponding gas phase values.[23] These results are in agreement with those reported by Zhou *et al.*[24] The observation that the C–Br stretch frequency is decreased by nearly 10 meV from its gas phase value, but that the C–H vibrational frequencies are not significantly altered supports the conclusion that CH_3Br is bonded to the Pt substrate through the Br and not through the hydrogens. Additional loss peaks at 118 and 179 meV (CH_3 bending modes) are observed in the specular direction, although these vibrational modes would be dipole forbidden in C_{3v} symmetry and only seen in the case of strong impact scattering. The observation that they are due to dipole scattering leads to the conclusion that the symmetry of the molecule is lower than C_{3v}. As Zhou *et al.*[24] have already suggested, this can be interpreted as an adsorption

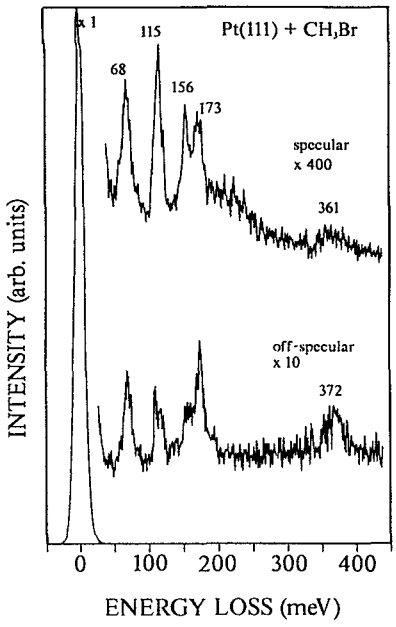

FIG. 5. HREEL spectra of monolayer CH_3Br (top) specular and (bottom) 15° off-specular.

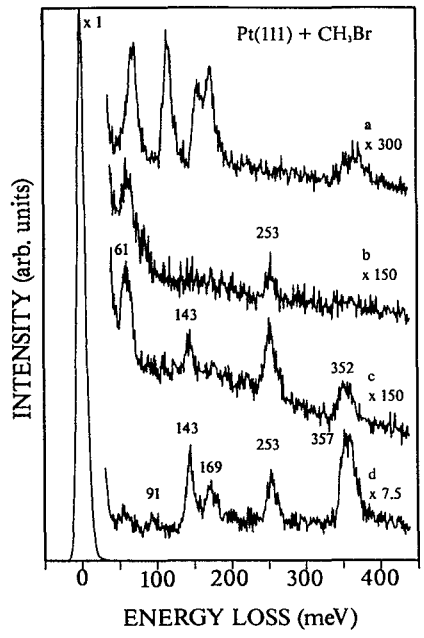

FIG. 6. HREEL spectra of (a) chemisorbed CH_3Br, specular, (b) after 40 min of UV irradiation, specular, and (c) and (d) both measured after annealing to 255 K; (c) specular and (d) off-specular.

geometry with the CH_3–Br axis tilted with respect to the surface normal.

2. CH_3

Shown in Figs. 6(b)–6(d) are HREEL spectra following illumination of chemisorbed CH_3Br. Figure 6(b) shows the spectrum of an unannealed sample, measured at the specular angle directly after 40 min illumination, as in Fig. 2. Figures 6(c) and 6(d) show HREEL spectra after annealing the sample at 255 K to remove any readsorbed CH_3Br. The spectrum (c) that was measured at the specular angle shows distinct loss peaks at 61 meV, 143 meV, and a broad peak around 352 meV. In addition, there is an indistinct shoulder in the elastic peak at ~23 meV. The HREEL spectrum (d) measured 15° off-specular has, in addition to all the loss features observed through dipole scattering at the specular angle, three additional loss peaks at 91, 169, and 357 meV. Noting the work of Ceyer *et al.*[25] on the dissociative chemisorption of CH_4 on Ni{111}, we can assign the loss features at 61 and 143 meV, seen in dipole scattering, to the Pt–CH_3 stretch and the CH_3 symmetric deformation, or umbrella mode, respectively. The broad peak at 352 meV may be assigned to the CH_3 symmetric stretch. The loss peak at 91 meV is most likely due to the low-frequency CH_3 rock, while the peaks at 169 meV and the broad peak at 357 meV are assigned to the CH_3 degenerate deformation and the CH_3 asymmetric stretch, respectively. All of the above loss frequencies are listed in Table I. The barely apparent feature at ~23 meV is due to the Pt–Br stretch of atomic bromine. The HREELS detection of the symmetric CH_3 vibrations in dipole scattering and the asymmetric CH_3 vibrations only in impact scattering indicate that the configuration of the CH_3 species produced through UV photon-induced fragmentation of chemisorbed CH_3Br on the Pt{111} is C_{3v}, i.e. the metal-C axis is perpendicular to the surface. Our results are to be contrasted with those of Costello *et al.*,[9] who observe the same spectrum in specular and off-specular and conclude that the symmetry of the CH_3 species is lower than C_{3v}.

TABLE I. Vibrational frequencies of CH_3Br and CH_3.

Vibrational modes of CH_3Br/CH_3	CH_3Br gas phase[a] E, meV (cm^{-1})	CH_3Br on Pt{111}[b] E, meV (cm^{-1})	CH_3 on Pt{111}[b] E, meV (cm^{-1})
ν_3 (A_1)			
C–Br stretch	76 (611)	68 (548)	···
ν_6 (E)			
CH_3 rock	118 (955)	115 (927)	91 (734)
ν_2 (A_1)			
CH_3 s deform	162 (1306)	156 (1258)	143 (1153)
ν_5 (E)			
CH_3 d deform	179 (1443)	173 (1395)	169 (1363)
ν_1 (A_1)			
CH_3 s stretch	364 (2935)	···	352 (2839)
ν_4 (E)			
CH_3 d stretch	379 (3056)	361 (2911)	357 (2879)
ν			
Pt–CH_3 stretch	···	···	61 (492)

[a] Reference 20 (IR).
[b] This work (HREELS).

3. HBr

The loss feature at 253 meV that appears in all the spectra after long illumination times still has to be assigned. A peak near 255 meV in such a situation is likely to be due to the C–O stretching frequency. This would be consistent with the HREELS data presented in Fig. 2, where it can be seen that, although the peak at 253 meV is hardly visible at short illumination times (up to 20 min), after longer illumination times of 40 and 80 min, corresponding to the almost complete removal of CH_3Br from the Pt surface, its intensity increases considerably. However, since HBr is observed in the TDS measurements following UV illumination, it was possible that this peak might result from the H–Br stretch, shifted to a considerably lower frequency in comparison to its value to the solid ($\sim$300 meV) (Ref. 26) and the gas phase ($\sim$317 meV).[27] Direct adsorption experiments with HBr were thus carried out.

The Pt{111} sample was first exposed to increasing concentrations of HBr at room temperature. HREEL spectra measured after various exposures to HBr showed no indication of any loss peak that could be identified with the H–Br stretch. The only feature observable is an unresolved shoulder in the elastic peak due to the Pt–Br stretch. These observations are indicative of dissocative adsorption of HBr and are similar to the results of Wagner and Moylan[28] in their HREELS study of HCl on Pt{111}. In addition, it is worth noting that no loss peak is observed at 253 or 255 meV, which suggests that the loss peak at 253 meV was not due to HBr, but in fact to CO. A peak of this intensity corresponds, however, to a CO coverage of considerably less than a tenth of a monolayer.

Since hydrogen is known to desorb at around room temperature on this surface, HREEL spectra were measured at 150 K in the specular and off-specular (15°) directions for the Pt{111} sample exposed to 60 L HBr. In both spectra, an unresolved shoulder at 23 meV due to the Pt–Br stretch is observed. In addition, the HREEL spectrum in the specular direction shows two broad losses at 54 and 136 meV. In the off-specular direction, loss peaks at 64 and 136 meV with intensities comparable to those of the losses in the specular direction are observed. Comparison with the HREEL spectra of pure hydrogen on Pt{111} shows that the features are very similar. The fact that H has a very low scattering cross section explains the similar intensities of losses in the specular and off-specular directions. The loss peak at 136 meV is attributed to the perpendicular mode of H against the Pt{111} surface, which is also the dipole active mode. In addition, there are two degenerate modes of H parallel to the surface when it is adsorbed in a threefold site. The loss peaks at 54 and 64 meV are attributed to these parallel modes whose degeneracy may be lifted due to H–H or H–Br interactions. These spectra clearly indicate that at low temperatures HBr also adsorbs dissociatively, similar to the situation at room temperature, but with the difference that below the desorption temperature of H_2 the Pt–H modes can clearly be observed.

To determine whether there is any reaction at all between Br and H coadsorbed on the surface, a predominantly Br covered surface was first prepared by exposing the Pt{111} surface to 60 L HBr at 150 K, followed by heating to 540 K, where thermal desorption of HBr in the CH_3Br experiments was observed, and then cooling to 150 K again. Cooling to 150 K appears to result in some H_2 readsorption. This surface was then exposed at 150 K to 2000 L of H_2 and HREEL spectra measured both in the specular and off-specular directions. Spectra identical to those in Fig. 7 were obtained, with no indications of any new loss features. These experiments show that Br and H do not react on the Pt{111} surface at temperatures lower than room temperature, even in the presence of excess H_2. The formation of HBr in the photon-induced reaction seems to be due to the secondary reaction of Br with CH_x species from the CH_3Br, rather than the reaction of Br with surface or gas phase H atoms.

This latter conclusion is supported by the HREEL spectra shown in Fig. 8. These were measured as a function of annealing temperature in order to monitor the vibrations of species remaining on the Pt surface during sequential desorption. The first two spectra from the top show once again the parent CH_3Br molecule before and after 40 min of illumination, both at 148 K. On sequential annealing to higher temperatures, several interesting observations may be made. The loss peak at 143 meV corresponding to a CH_3 bending mode, seen at 255 K, disappears on annealing to 325 K. This seems to correlate with the detection of CH_4 in TDS at 275 K in our experiment and with the suggestion of White *et al.* in their study[9] that CH_4 is formed through the dehydrogenation of two CH_3 groups on the Pt surface. In addition, it should be noted that, even after removal of CH_3 as CH_4 at 325 K, the loss peak at 357 meV corresponding to a C–H stretch still remains, indicating the added presence of either CH_2 or CH on the surface. This peak is seen in EELS until a temperature of 600 K is reached. However, beyond 600 K, no C–H stretch is observed, and finally on annealing to 700 K, no loss peaks can be seen apart from an unresolved shoul-

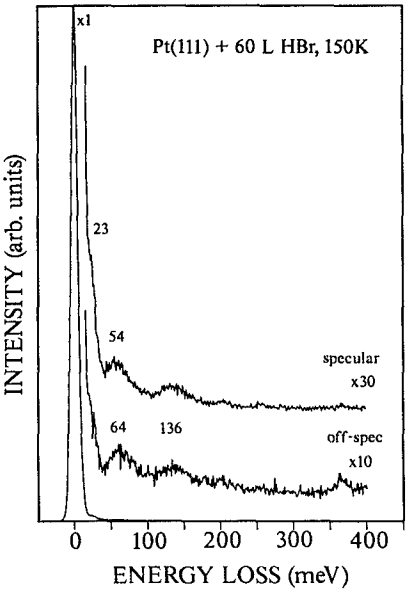

FIG. 7. HREEL spectra of 60 L HBr adsorbed at 150 K on Pt{111} measured in both specular and 15° off-specular directions.

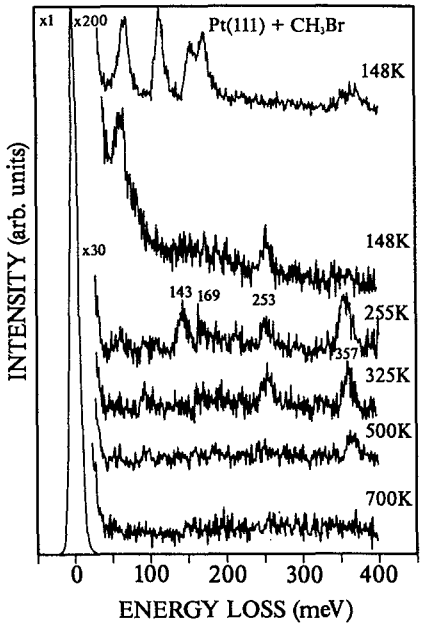

FIG. 8. HREEL spectra measured as a function of annealing temperature in order to monitor secondary reaction products on the surface. From top to bottom: chemisorbed CH_3Br before and after 40 min of UV irradiation, both measured at 148 K in the specular direction. Subsequent annealing to 255, 325, 500, and 700 K measured 15° off-specular.

der in the primary peak corresponding to the Pt–Br stretch. Since HBr desorbs at 540 K, the disappearance of the C–H stretching frequency above 600 K suggests that the formation of HBr occurs at these high temperatures through a secondary reaction of Br with CH_2 and CH.

E. Fragmentation mechanisms

The absorption spectrum of CH_3Br in the gas phase is continuous in the region 180–285 nm, with a maximum at 205 nm (6.05 eV).[21] This absorption is attributed to an $n\rho_\pi \rightarrow \sigma^*$ transition of the nonbonding electrons localized on the Br atom into the lowest antibonding σ orbital associated with the C–Br bond. There is no reported absorption at wavelengths longer than 285 nm. While the photolysis of CH_3Br in the gas phase has been studied at 185 nm, producing CH_3 and Br with unit quantum efficiency,[29] no measurements appear to have been made at other wavelengths. Since unit quantum efficiency in the free molecule is a reasonable assumption over the whole spectral range investigated, we are justified in comparing the two curves in Fig. 4. In contrast to the gas-phase absorption curve, which does not extend beyond 285 nm, the fragmentation curve for chemisorbed CH_3Br is quite broad, and extends up to nearly 400 nm. The fragmentation curve of chemisorbed CH_3Br shows a maximum around 330–340 nm ($\sim$3.7 eV), also red-shifted by about 130 nm ($\sim$2 eV) from the gas-phase maximum. Additionally, the cross section at the maximum in our experiment is about an order of magnitude lower than the absorption cross section at the gas-phase maximum of 205 nm.[22]

Following recent discussions in the literature there are two possible mechanisms, both of which can explain the observed red-shift. The first is a direct electronic excitation in the chemisorbed CH_3Br to a repulsive state CH_3Br^* that can undergo nuclear motion leading to dissociation. The chemisorptive interaction between the CH_3Br^* and the Pt could result in a lowering of the energy of the optical excitation, leading to the red-shift. The second possibility involves photon absorption by the Pt substrate, leading to the production of primary and secondary electrons. Subsequent capture of such a "hot" electron by the σ^* orbital gives rise to dissociation. A red-shift would arise from the fact that the threshold for such an excitation is given by the difference in energy between the Fermi level and the σ^* orbital, which is necessarily smaller than the optical excitation energy in the molecule.

Although the present data cannot unequivocally prove the dominance of one or the other mechanism, the observation of a maximum in the measured fragmentation curve strongly suggests a specific electronic excitation. If the mechanism were to involve substrate excitation of hot electrons, one would instead expect a monotonic increase in the fragmentation cross section with decreasing wavelength, since the increasing number of secondary electrons would lead to a corresponding increase in the probability of electron attachment. The only possibility of obtaining a maximum within the framework of a hot electron mechanism would be from some specific wavelength-dependent structure in the substrate absorption spectrum. This can, however, be ruled out by calculating the fraction of incident energy absorbed using the Fresnel formulas in conjunction with literature data[30] for the dielectric function. The resulting curve increases almost linearly with photon energy (Fig. 9) and hence cannot cause any structure in the fragmentation cross section.

This latter result would seem to favor the direct excitation mechanism. We can, however, obtain some indirect information on the energy of this transition by measuring the photoelectron spectrum of CH_3Br adsorbed on Pt{111}. The gas-phase photoelectron spectrum of CH_3Br has been recorded by Brogli and Heilbronner[31] and shows the two spin-orbit split nonbonding states at binding energies of 10.53 and 10.85 eV. In the corresponding spectrum of the

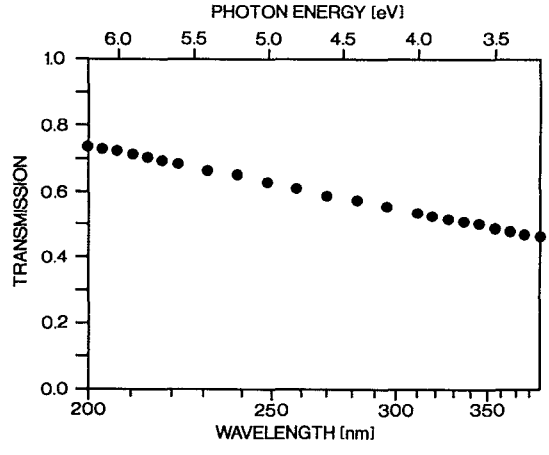

FIG. 9. Transmission, T, of a Pt surface as a function of photon energy at normal incidence. $T = 1 - R$, where R is the reflectivity.

adsorbed species in Fig. 10 these orbitals are found (unresolved) at a binding energy of about 5 eV with respect to the Fermi level. The reported electron affinity of CH_3Br in the gas phase is 0.4 eV,[32] which gives some indication of the position of the σ^* (C–Br) antibonding level in the free molecule. On chemisorption this level will be broadened and shifted toward the Fermi level. Unfortunately, no experimental data from inverse photoemission are available to give a more precise characterization of the spectral density above the Fermi level. We can, however, draw some conclusions already from the photoemission results if we consider the final state in this experiment to be fully relaxed. Even on the assumption that the affinity level in chemisorbed CH_3Br extends down to the Fermi level the intramolecular excitation energy cannot be lower than the binding energy of the lone pair orbitals, as measured in photoemission. Since both the onset ($\sim$3.2 eV) and the maximum (3.7 eV) of the fragmentation curve (Fig. 4) are clearly below this limit we must exclude the $np_\pi \rightarrow \sigma^*$ transition in the chemisorbed molecule as the origin of the photon-induced dissociation. We suggest instead a charge transfer process as the primary step in which electrons from the *d* bands of Pt are excited into the σ^* (C–Br) orbital above the Fermi level. The dissociating species will then be a negatively charged CH_3Br molecule created via this electron attachment process. Such a dipole excitation can become possible through mixing of the unoccupied σ and metal states due to the chemisorption interaction. The transition probability depends on both the density of the occupied *d* band (initial states) and the σ^* final state as well as on the transition matrix element. The density of *d* states is already strongly modulated, as is evident from the UV photoemission spectra (Fig. 10), which alone could account for the observed structure in the fragmentation curve. In this model we can identify the onset of dissociation with excitations of electrons from the Fermi edge and can tentatively place the σ^* orbital of the adsorbed CH_3Br molecule about 3 eV above the Fermi level. Inverse photoemission experiments would clearly be useful for comparison.

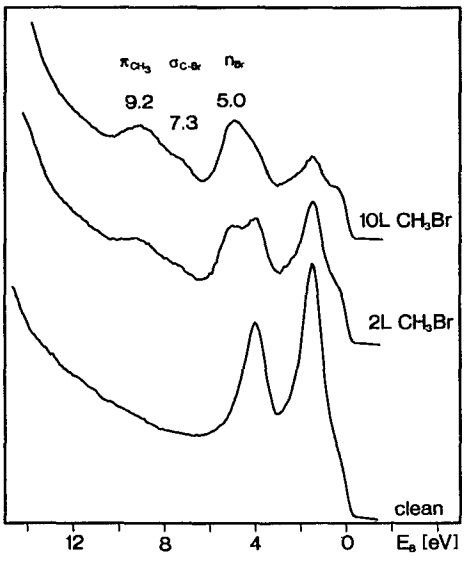

FIG. 10. He I photoemission spectra of the adsorption of CH_3Br on Pt{111}. Adsorbate-induced features are observed at binding energies of 5.0, 7.3, and 9.2 eV, corresponding to the np_π (Br), σ(C–Br), and $\pi(CH_3)$ orbitals, respectively.

IV. SUMMARY AND CONCLUSIONS

The results of this study of the photon-induced reactions of chemisorbed CH_3Br on Pt{111} may be summarized as follows:

A quantitative measurement of the fragmentation cross section of chemisorbed CH_3Br has been made. The long-wavelength limit of this curve as well as the maximum at $\sim$3.7 eV is redshifted by about 2 eV with respect to the corresponding gas-phase absorption limit. The shape of the fragmentation curve is suggestive of dissociation induced by electron attachment via charge transfer excitations.

Both primary and secondary reactions have been identified. The primary photoreaction initiated by UV results in the production of CH_3 and Br. A secondary surface reaction occurs between Br and CH_2 and/or CH at higher temperatures, resulting in the production of HBr.

The CH_3 species has been characterized by HREELS and is found to have C_{3v} symmetry.

ACKNOWLEDGMENTS

This work has been supported by the Deutsche Forschungsgemeinschaft through the Sonderforschungsbereich 6.

[1] J. R. Swanson, C. M. Friend, and Y. J. Chabal, J. Chem. Phys. **87**, 5028 (1987).
[2] J. R. Creighton, J. Vac. Sci. Technol. A **4**, 669 (1986).
[3] E. B. D. Bourdon, J. P. Cowin, I. Harrison, J. C. Polanyi, J. Segner, C. D. Stanners, and P. A. Young, J. Phys. Chem. **88**, 6100 (1984).
[4] F. L. Tabares, E. P. Marsh, G. A. Bach, and J. P. Cowin, J. Chem. Phys. **86**, 738 (1987).
[5] F. A. Houle, Chem. Phys. Lett. **95**, 5 (1983).
[6] C. E. Bartosch, N. S. Gluck, W. Ho, and Z. Ying, Phys. Rev. Lett. **57**, 1425 (1986).
[7] M. A. Henderson, G. E. Mitchell, and J. M. White, Surf. Sci. **184**, L325 (1987).
[8] B. Roop, K. G. Lloyd, S. A. Costello, A. Campion, and J. M. White, J. Chem. Phys. **91**, 5103 (1989).
[9] S. A. Costello, B. Roop, Z. M. Liu, and J. M. White, J. Phys. Chem. **92**, 1019 (1988).
[10] K. G. Lloyd, B. Roop, A. Campion, and J. M. White, Surf. Sci. **214**, 227 (1989).
[11] E. P. Marsh, M. R. Schneider, T. L. Gilton, F. L. Tabares, W. Meier, and J. P. Cowin, Phys. Rev. Lett. **60**, 2551 (1988).
[12] E. P. Marsh, T. L. Gilton, W. Meier, M. R. Schneider, and J. P. Cowin, Phys. Rev. Lett. **61**, 2725 (1988).
[13] T. J. Chuang and K. Domen, J. Vac. Sci. Technol. A **5**, 473 (1987).
[14] B. Roop, S. A. Costello, C. M. Greenlief, and J. M. White, Chem. Phys. Lett. **143**, 38 (1988).
[15] X. Y. Zhu, S. R. Hatch, A. Campion, and J. M. White, J. Chem. Phys. **91**, 5011 (1989).
[16] J. R. Creighton, J. Appl. Phys. **59**, 410 (1986).
[17] N. S. Gluck, Z. Ying, C. E. Bartosch, and W. Ho, J. Chem. Phys. **86**, 4957 (1987).
[18] E. Hasselbrink, S. Jakubith, S. Nettesheim, M. Wolf, A. Cassuto, and G. Ertl, J. Chem. Phys. **92**, 3154 (1990).
[19] G. Radhakrishnan, W. Stenzel, H. Conrad, and A. M. Bradshaw, Appl. Surf. Sci. **46**, 36 (1990).
[20] R. Unwin, W. Stenzel, A. Garbout, H. Conrad, and F. M. Hoffmann, Rev. Sci. Instrum. **55**, 1809 (1984).
[21] H. Okabe, *Photochemistry of Small Molecules* (Wiley, New York, 1978), p. 301.

[22] G. N. A. Van Veen, T. Baller, and A. E. De Vries, Chem. Phys. **92**, 59 (1985).
[23] T. Shimanouchi, *Tables of Molecular Vibrational Frequencies*, NSRDS-NBS 39, Washington D.C., 1972, Vol. 1, p. 54.
[24] Y. Zhou, W. M. Feng, M. A. Henderson, B. Roop, and J. M. White, J. Am. Chem. Soc. **110**, 4447 (1988).
[25] M. B. Lee, Q. Y. Yang, and S. T. Ceyer, J. Chem. Phys. **87**, 2724 (1987).
[26] D. F. Hornig and W. E. Osberg, J. Chem. Phys. **23**, 662 (1955).
[27] J. M. Cherlow, H. A. Hyatt, and S. P. S. Porto, J. Chem. Phys. **63**, 3996 (1975).
[28] F. T. Wagner and T. E. Moylan, Surf. Sci. **216**, 361 (1989).
[29] P. C. Kobrinsky and R. M. Martin, J. Chem. Phys. **48**, 5728 (1968).
[30] *Physik Daten, Optical Properties of Metals*, Part. 1, edited by H. Behrens and G. Ebel (Fachinformationszentrum, Karlsruhe, 1981), Vol. 18-1, p. 282.
[31] F. Brogli and E. Heilbronner, Helv. Chim. Acta **54**, 1423 (1971).
[32] *Reference Data on Atoms, Molecules, and Ions*, edited by A. A. Radzig and B. M. Smirnov (Springer-Verlag, Berlin, 1985), p. 436.